**LUNAR BOULDERS SEEN AT VERY HIGH RESOLUTION: IMPLICATIONS FOR 433 EROS.** B. Wilcox[1], M.S. Robinson[1], P.C. Thomas[2], [1]Northwestern University 1847 Sheridan Rd. Evanston, IL, 60208, [2]Cornell University, Ithaca, NY 14853.

**Introduction:** NEAR MSI images show abundant evidence that the surface of 433 Eros is covered in a loose fragmental layer of unconsolidated debris [1,2,3,4] known as a regolith. A striking characteristic of the regolith is a geographically distinctive population of blocks that range in size up to 150 m in diameter [3]. Simulations of ejection trajectories from the largest craters on Eros led [3] to the conclusion that the majority of blocks (diameters >15 m) on Eros were emplaced as a result of the formation of Shoemaker crater (SC). Several unanswered questions remain concerning the blocks on Eros. Is their apparent high population density (inside and outside SC) consistent with the hypothesis that they indeed are a product of the formation of SC? If so why do we not find boulder populations related to other large craters on Eros (i.e. Selene, Psyche, Himeros)? Can we identify boulder populations at small scales (sub-meter resolution) that can be related to small craters? If so can estimates of regolith depth be made? To investigate these questions we have studied 150 very high resolution (~1 m/pixel) Lunar Orbiter (LO) frames keying on the identification and spatial relations of boulders and craters. We extend previous studies of lunar blocks that date to the earliest days of lunar exploration [5,6] and have been used to infer properties of the regolith, and type of impactor (primary or secondary) [5,6,7,8,9].

**Data:** Lunar Orbiter images were chosen for the study because of their high resolution, ideal lighting conditions (69°-73° inc.), and their fairly broad sampling of the surface. All but a few of the LO images cover mare regions, thus sampling portions of the Moon thought to have the shallowest regolith [7]. The selected LO images were digitally scanned into a common format accessible to an interactive monitor/cursor digitizing program developed especially for this project. Thus far we have collected two datasets from the LO images; digitization of block populations in and around parent craters, and a count of craters with block populations per unit area.

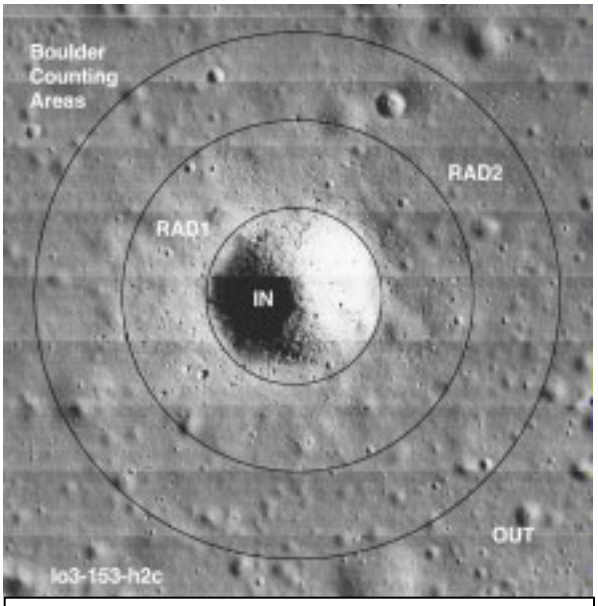


**Figure 1. Illustration of Boulder counting areas, radius of crater is ~260 m (LO3-153-H2c see also [10]).**

**Blocky Crater Populations:** To quantify the frequency of blocky craters we identified all craters with diameters larger than 100 m and classified them according to number and spatial distribution of blocks. We note that LO images were generally selected on the criteria that they had craters with boulders, thus the results presented here represent an upper limit for the distribution of bouldery craters. Our study area (~ lat. 1°S to 4°S, lon. 42°W to 45°W) is contained within the large (~50 km diameter) mare flooded crater near Flamsteed, from 12 LO images we identified 213 craters greater than 100 meters in diameter, in a total area of 124 km$^2$. Mapped crater diameters range from 100 to 1700 m, with an average diameter of 185 m. We find it significant that over half of the mapped craters are boulderless (H) and that 88% have no boulders to just a few boulders (H plus F); note that with class F it is not clear that the few boulders found are actually related to that particular crater. Craters with abundant boulders are rare (3%, classes A and B). We find it significant that craters of the same size and same degradation state can be found in close spatial proximity with vastly different boulder populations.

| Class | Craters/ 100 km$^2$ | % total craters |
|---|---|---|
| ABCDEFH | 171.1 | 100 |
| ABCD | 20.1 | 12 |
| AB | 5.6 | 3 |
| ABCDEF | 77.9 | 45 |
| HF | 151.0 | 88 |
| H | 93.2 | 55 |

**Table 1.** *Summary of abundance of craters greater than 100 m diameter found in study area. Class shows a progression of boulders per crater, with A having the greatest number to H having no more than 1 boulder.*

**Block Distribution:** We identified all craters with blocks and classified them according to spatial characteristics of the blocks relative to their parent crater. We have thus far digitized all blocks around representatives of four classes of craters (those with highest density of boulders). The position and diameter of all blocks were recorded by fitting a circle to three points around each block. Possible sources of error in this process include the difficulty in fitting a circle to the actual block shape, resolution effects as block size approaches the limit of image resolution, and the obscuration effects of saturated and shadowed portions of a crater (such areas were excluded). For each block population we calculated a reverse cumulative histogram and found the slope of best line to the population on the basis of five geographic units for each crater (see caption **Table 3**). Cumulative slopes steeper than –2 represent heavily fragmented materials [**9**].

| Class | area ($km^2$) | % total area |
|---|---|---|
| ABCDEF ($\pi r^2$) | 9.3 | 7.5 |
| ABCD ($\pi r^2$) | 4.6 | 3.7 |
| AB ($\pi r^2$) | 4.0 | 3.3 |
| *AB ($\pi d^2$), CD ($\pi r^2$)* | *16.8* | *13.5* |
| *AB ($\pi d^2$)* | *16.2* | *13.0* |

**Table 2.** *Summary of areal coverage of boulder fields in the study area (124 $km^2$). Only classes A and B have abundant boulders exterior to the crater; thus the last two rows (italics) include areas outside of crater out to one radii from rim for A and B.*

During boulder identification we frequently observed that angular to subangular boulders are often found on what appear to be relatively degraded craters (those that do not exhibit a crisp rim). The most reasonable explanation is that the near-surface material is extremely weak (comminuted regolith) and thus a crisp rim is never formed. We also did not find any sign that boulders had rolled or slid down crater walls after emplacement (boulder tracks).

**Discussion:** The production of ejecta on different solar system bodies is thought to be similar, despite gravitational and compositional differences [**8**]. Further, comparisons between mare and highland craters of a given diameter show that the mean block size does not appear dependent on the nature of the material impacted (for craters above 100m). A relationship between regolith thickness and block density within 1.1 radii of crater centers was demonstrated by Cintala and McBride (1995); regolith thickness was estimated by apparent strength discontinuities (QO) inside craters [**6**]. In our study area we find craters of like size and degradation state with a large range of boulder densities and SD craters near 'normal' craters. This indicates that the regolith is highly variable in thickness or other factors (impact velocity?) are equally important in boulder and QO crater generation. Thus far our analysis of lunar boulders has shown that the boulder distribution slope for SC on Eros is consistent with lunar craters (in agreement with [**7-10**]), and that it is not unexpected that some craters on Eros have boulders and some do not. In fact from the lunar example it is apparent that bouldery craters make up far less than 50% of the population of 100 m and larger craters (at a scale of ~1m/p) on the Moon. Future work will include digitization of more boulders around craters, as well as an extension of the areal coverage of bouldery crater populations, with extension into the highlands.

| crater | class | diam | all | in | rad1 | in+rad1 | rad2 | n |
|---|---|---|---|---|---|---|---|---|
| LO3-153-H2c | A | | -3.41 | -3.11 | -3.16 | -3.36 | -3.29 | 10,087 |
| LO2-104-H3 | B | | -3.54 | -2.81 | -3.02 | -3.50 | n/a | 1083 |
| LO2-070-H1 | C | | -3.95 | -3.85 | -3.71 | -3.95 | n/a | 3444 |
| LO3-159-H3 big | D | | *-2.33* | -2.10 | -2.14 | -2.09 | -1.89 | 508 |
| LO3-159-H3 small | D | | *-2.33* | -3.10 | n/a | -2.92 | n/a | 165 |
| LO3-197-H1b | D | | -2.49 | -2.62 | -1.55 | -2.49 | n/a | 165 |
| LO#-209-H2right | D | | -2.52 | -2.30 | -2.92 | -2.52 | n/a | 620 |

**Table 3.** Summary of boulder population per crater. Crater diameter reported in meters, slope values are presented according to geographic distribution: *all* – within 3 radii of center, *in* – all inside crater, *rad1* – between rim and one crater radius of the rim, *rad+in* – all boulders found inside the crater and out to one radius from the rim, *rad2* – all boulders found between one and two radii of the rim, *n* – the total number of boulders associated with a particular crater. Note that for LO3-159-H3 the two craters shown are side by side thus knowledge of which boulder actually was produced by which crater is not possible, the *all* category in this case is a combination of both craters. Boulders for crater LO3-153-H2c (**Fig. 1**, Type) were also digitized by [**10**] and our results compare favorably with theirs.

**References:** [**1**] Veverka et al. (2000), *Science*. 289, 2088-2097. [**2**] Veverka et al. (2001), *Nature*, 413, 390-393. [**3**] Thomas et al. (2001), Nature, 413, 394-396, [**4**] Robinson et al. (2001), *Nature*, 396-400. [**5**] Shoemaker et al (1967) *JPL Tech. Rept. 32-1177*, 9-67. [**6**] Quaide and Oberbeck (1968), JGR, 73, 5247-5270. [**7**] Cintala and McBride (1995), *NASA Tech. Memo.* 104804, 441 pp. [**8**] Lee et al. (1986), *Icarus*, 68, 77-86. [**9**] Hartman (1969), *Icarus*, 10, 201-213. [**10**] Cintala et al. (1982) *LPS XIII* (abstract), 100-101.